Correlation between nuclear stopping and directed flow at intermediate energy

Dissertation submitted in the partial fulfillment of the requirement for

The award of the degree of

Master of Science

in

Physics

Submitted by

Yoshita Ahuja

Roll No- 301004019

Under the guidance of

Dr. Suneel Kumar

School of Physics and Material science

Thapar University

Patiala – 147004 (PUNJAB)

INDIA

Dedicated

TO

My Family

CERTIFICATE

This is certifying that Ms. Yoshita Ahuja, Roll No. 301004019 has worked on this dissertation as a partial fulfillment for award of the degree of MASTERS OF SCIENCE in Physics. I certify that the matter embodied in this dissertation is the candidate's own record and not submitted to any other university in any part or full form for the award of such a degree.

S Kumar

(Dr. Suneel Kumar)
Associate Professor
School of Physics and Material Science
Thapar University, Patiala

Countersigned by:

Dr. Kulvir Singh
(Head)
School of Physics and Material Science
Thapar University, Patiala

Dr. S.K. Mohpatra
Dean of academic Affairs
Thapar University, Patiala

ACKNOWLEDGEMENT

Knowledge in itself is a continuous process. I would have never succeeded in completing my task without cooperation, encouragement and help provided to me by various personalities.

My foremost thanks goes to my worthy supervisor **Dr. Suneel Kumar**. Without him, this dissertation would not have been possible. I thank him for his patience and encouragement that carried me on through difficult times, and for his insights and suggestions that helped to shape my research skills. I express my sincere thanks to him for his valuable guidance in carrying out work under his effective supervision, encouragement and cooperation. His visionary thoughts have influenced me greatly.

I also thank **Dr. Kulvir Singh**, head, School of Physics and Materials Science for his support and providing facilities.

I wish to express my thanks to **Miss Anupriya Jain**, Research Scholars for the help and valuable suggestions whenever I needed out of their busy schedule.

All my friends and the staff at the School of Physics and Materials Science are acknowledged for providing me a friendly atmosphere and encouraging me throughout this work. Their assistance and partnership were of great pleasure. Their views were very insightful and helpful. I am deeply thankful to my family, their moral support and patience has bared fruit through completion of this dissertation which will result in award of the prestigious degree of M.Sc. in Physics.

Above all I render my gratitude to the Almighty who bestowed self- confidence, ability, strength and path to me in accomplishing this work.

Yoshita Ahuja

Date- 29-06-2012

Yoshita Ahuja

Place- Thapar University,

Roll No: 301004019

Patiala.

Abstract

The present work deals with the theoretical study of nuclear stopping and its correlation with directed flow in heavy-ion collision at intermediate energy. We present a complete systematic of nuclear stopping and directed flow for symmetric colliding nuclei in the energy range between 100 MeV/nucleon and 600 MeV/nucleon by using soft equation of state. This study is performed within an isospin dependent quantum molecular dynamics (IQMD) model. The effect of isospin dependent and isospin independent cross-section has also been studied and compared. A linear relation has been found between the stopping and directed flow.

Table of contents

List of figures

Chapter 1

INTRODUCTION

1.1 Heavy ion physics

The term heavy ion is generally used for the nuclei which are heavier than the helium nucleus. The heavy ion physics mainly concerns on the investigation of properties of nuclear matter at extreme densities and temperature [1-3]. Structure of nucleus, interactions among nucleons, nucleon-nucleon scattering as well as structure of nucleons are some of the properties of nuclear matter. Nuclear equation of state and liquid gas phase are known as bulk properties of nuclear matter which are very helpful in understanding the phenomena's like origin of early universe and supernova explosions etc. [4].

The heavy ion physics classified into mainly three groups :

1. Low Energy Heavy Ion Physics (E < 10 MeV/nucleon).
2. Intermediate Energy Heavy Ion Physics (10 MeV/nucleon < E < 2 GeV/nucleon).
3. High Energy Heavy Ion Physics (E > 2 GeV/nucleon).

The study at low energy nuclear physics is to look for the low density phenomena. The low energy nuclear physics mainly focus on structure of nuclei, fusion and fission. Due to the lack of free phase space available at low incident energy, about 98% of the attempted collisions are blocked. Thus, dynamics at low energies is governed by the mean field [5] only.

Intermediate energy nuclear physics gives the possibilities to study the properties of nuclear matter under extreme conditions. The properties of nuclear matter, like all other materials, are also influenced by the pressure, density, and temperature. The various phenomena's that we study at intermediate energy nuclear physics are collective flow, multifragmentation, nuclear stopping etc. [6].

In intermediate energy physics, both mean field and nucleon-nucleon collision takes place. Reactions at intermediate energy are violent enough to excite the system to very high

temperature leading to the break-up of initial correlations among nucleons, but not enough to break the internal structure of nucleons or hadrons.

But in high energy nuclear physics, at very high densities and temperatures, one may have the quark gluon plasma [7]. The availability of large free phase-space at high energy makes the Pauli blocking role quite small (roughly 4% collisions are blocked) and hence the dynamics of a reaction is governed by the nucleon-nucleon collisions.

1.2 Phases of nuclear matter

As we know that water has three states. We find that the state of nuclear matter depends on temperature and density. In normal states at lowest energy, nuclei show liquid-like characteristics and have a density of 0.17 nucleons/fm^3. In more conventional units, this corresponding to 2.7×10^{17} kg/m^3, or 270 trillion times the density of liquid water.

The possible way to heat the nuclei to significant temperatures is by colliding them with other nuclei. The temperatures reached during these collisions are astounding. Nuclear scientists use millions of electron volts or MeV as a convenient energy unit because it is roughly the energy scale of nuclear processes. An average energy of 1MeV corresponds to a temperature of 1.2×10^{10} K the temperatures we can reach in nuclear collisions range upto 100 MeV and above. We don't have any direct way of measuring the state variables as temperature, pressure, and density. We need to determine them from observables such as:

1. The abundance of isotopes,
2. The population of excited nuclear states,
3. The shape of the energy spectra from nuclear collision remnants,
4. The production of particles such as pions.

Now during heavy ion collisions the thermodynamic state variables can be measured and we are beginning to pin down the critical point of the nuclear liquid-vapour phase diagram.

Information about the size of fragments produced when nuclear matter is near its critical point gives essential information about the nuclear equation of state.

The X-axis represents the normal density and temperature is shown on Y-axis. Nuclear matter can exist in different phases like liquid, hadron gas and quark gluon plasma phases depending upon temperature and density.

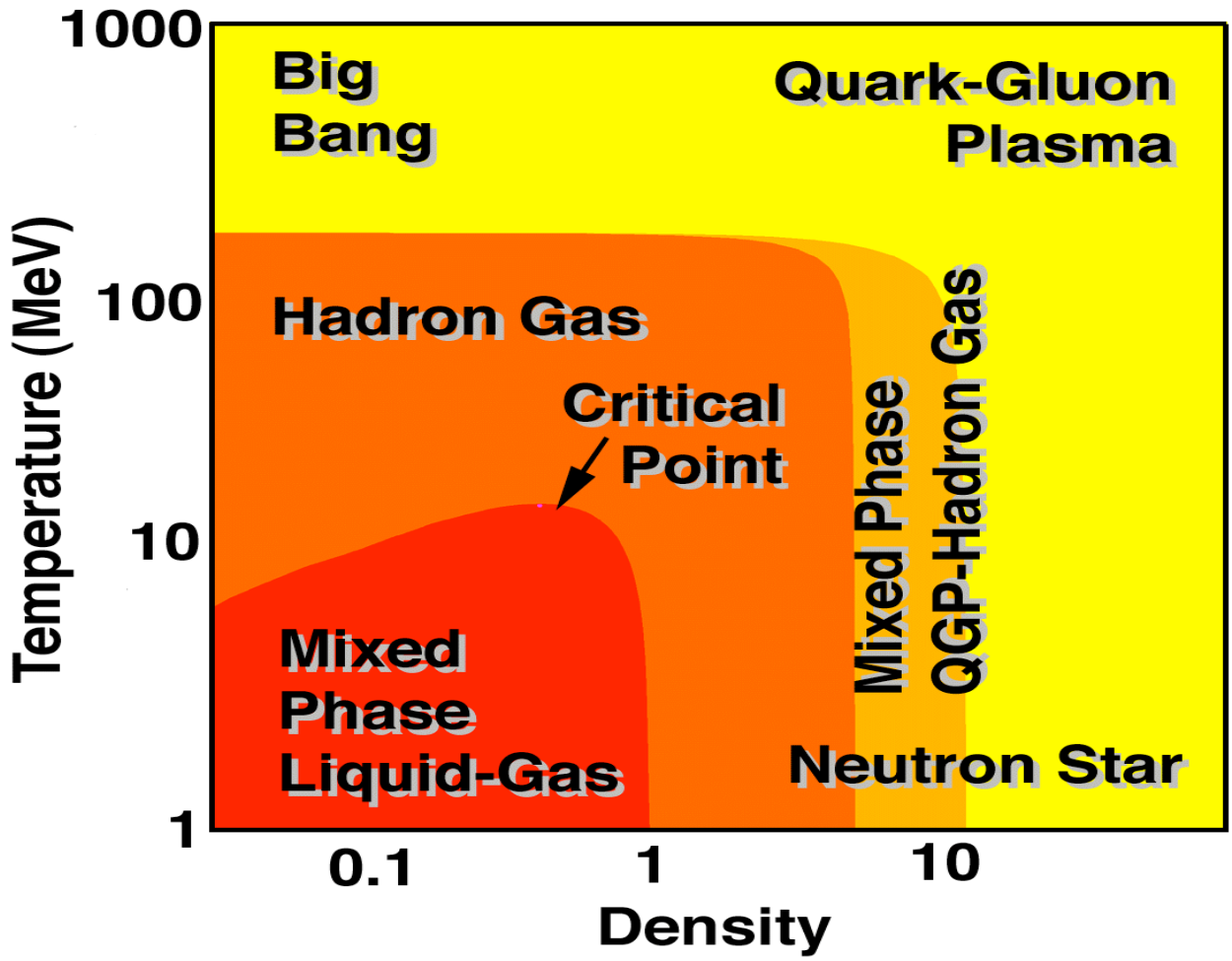

Fig.1.1 The phase diagram for nuclear matter, as predicted theoretically. The horizontal axis shows the matter density, and the vertical axis shows the temperature. Both axes are shown in logarithmic scale, and the density is given in multiples of normal nuclear matter density.

The normal nuclear matter at ($\rho=\rho_0$, T=0) represents the liquid phase. In Fig.1.1, the liquid gas phase (LGP) transition region at the lower left corner and is characterized by the temperature below ≈ 15 MeV and densities ($\frac{\rho}{\rho_0} < 1$). A highly dense and hot region corresponds to quark gluon plasma (QGP) phase. The Hadron gas (HG) phase exists at intermediate

temperature and density. The lines which separate the QGP phase from HG phase is the phase co-existance or transition region.

1.3 Purpose of studying the nuclear matter phase diagram

The purpose of studying nuclear matter phase diagram is to understand the early history of our universe, and to understand high-density objects, called "neutron stars" in our present day universe.

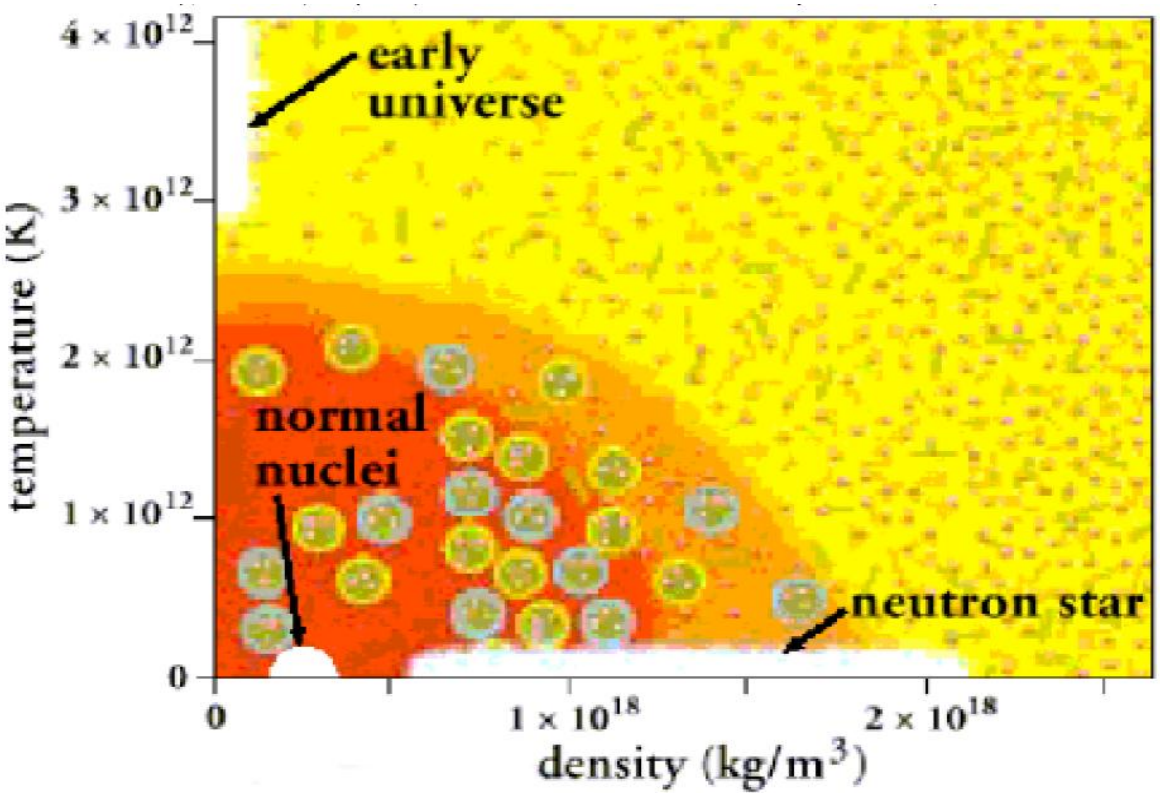

Fig 1.2 The quark-gluon plasma region shows the existence of quarks and gluons.

The upper left corner in Fig. 1.1 & Fig 1.2 is a region labeled "Big Bang". The Fig. 1.2, also show a region labeled "neutron star". When a massive star undergoes a supernova explosion, a core of nuclei remains. The short-range nuclear repulsive force is not strong enough to keep the nuclei apart. As the core collapses, the individual nucleons separate from the nucleus. The protons become neutrons by inverse beta decay. Therefore, the neutron star is very large collection of neutrons, typically a few kilometers in diameter, which is held together by gravity.

The study of the nuclear equation of state is connected to the initial phases of the early universe, to ultra-violet stellar explosions, and to experiments around the world. Heavy ion collision is one of the best tools for investigating the nuclear matter phase diagram. In the course of the collision, matter is compressed and heated up. Depending on initial conditions, various densities and temperatures can be reached and thus a large scale exploration of the nuclear matter phase diagram is possible. For example, the transition from hadronic matter to QGP is actively sought in today's experiments with ultra-relativistic heavy ions, at beam energies of several tens of GeV per nucleon. Hence heavy ion collisions seem to offer a unique opportunity for exploring the phase diagram of nuclear matter.

1.4 Study of different phenomenon at intermediate energies

a) Multifragmentation

It is the process [8] in which when two nuclei collide, during this collision they break into several small and medium sized fragments and lot of nucleons are emitted as shown in Fig. 1.3 The particles which are produced include the free nucleons (FN's) [A = 1], light charged particles (LCP's) [$2 \leq A \leq 4$] as well as heavy clusters.

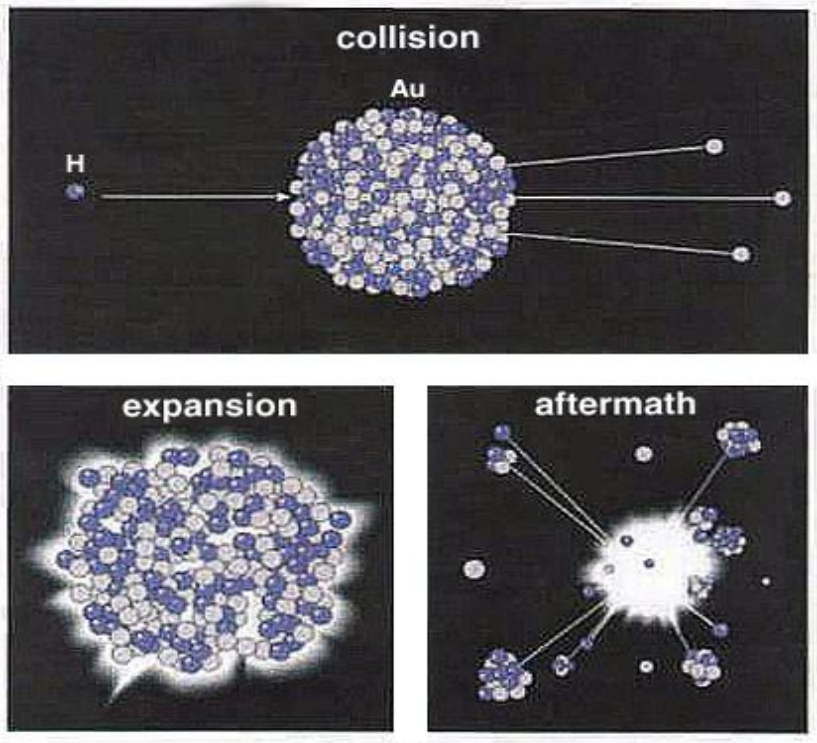

Fig. 1.3 Schematic view of the multifragmentation process.

b) Nuclear stopping

The study of heavy ion collisions at intermediate energy has been focused on variety of phenomenon and global stopping of nuclear matter [9] is one of them. Nuclear stopping is one of the essential observable of thermalization that depends crucially on reaction dynamics. It has been linked with the degree of thermalization and equilibrium reached in a reaction.

The establishment of radioactive beam facilities in many laboratories has enabled the study of neutron-rich (or proton-rich) nuclear collisions at intermediate energies. Besides the many existing radioactive beam facilities, many more are being constructed or under planning, including the cooling Storage Ring (CSR) facility at HIRFL in China, the Radioactive ion beam factory (RIBF) at RIKEN in Japan, the FAIR at GSI in Germany, GANIL in France, and Facility for Rare Isotope Beam (FRIB) in USA [10]. These facilities offer possibility to study the various phenomena. Among these phenomena, nuclear stopping of colliding matter has gained a lot of interest since it gives us possibility to examine the degree of thermalization or equilibration. It has been pointed out that [11] nuclear stopping at intermediate energies is determined by the mean field as well as by the in-medium nucleon-nucleon cross sections. The influence of the mean field is considered by taking the equation of state (EOS) to be "soft" EOS (κ = 200 MeV) and the "hard" EOS (κ = 380 MeV) as well as with and without the isospin symmetry potential.

Origin of nuclear stopping

If two nuclei collide three different scenarios are possible. These different scenarios are shown in Fig. 1.4 and are explained as follows:

1) The nuclei are repelled by each other like in the collision of two hard spheres. (shown in Fig. 1.4(a)).
2) The nuclei are compressed and mix-up like in the collision of two droplets (shown in Fig. 1.4(b)).
3) The nuclei are passing each other without much interactions like two large crowd of bees (shown in Fig. 1.4(c)).

c) Collective Flow

The collective flow is a measure of the transverse motion imparted to particles and fragments during the collision of two nuclei. The development of collective flow is closely related to the pressure build-up during the compression stage of the reaction, and gives us information about the pressure and particle density relation.

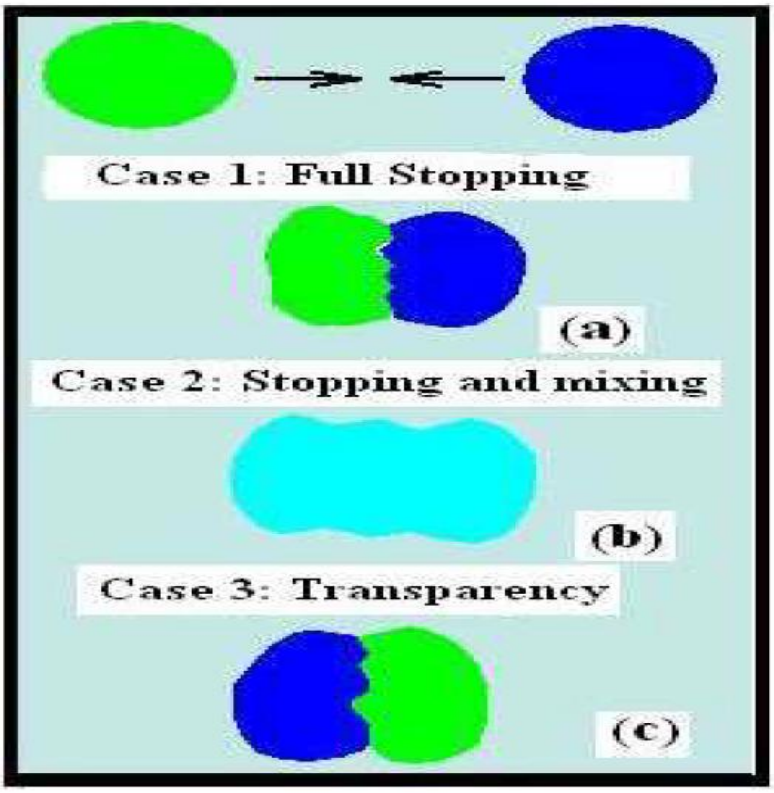

Fig. 1.4 Schematic movement of the projectile and target nucleons. The figure representing (a)Full stopping, (b) Stopping and mixing, (c) Transparency.

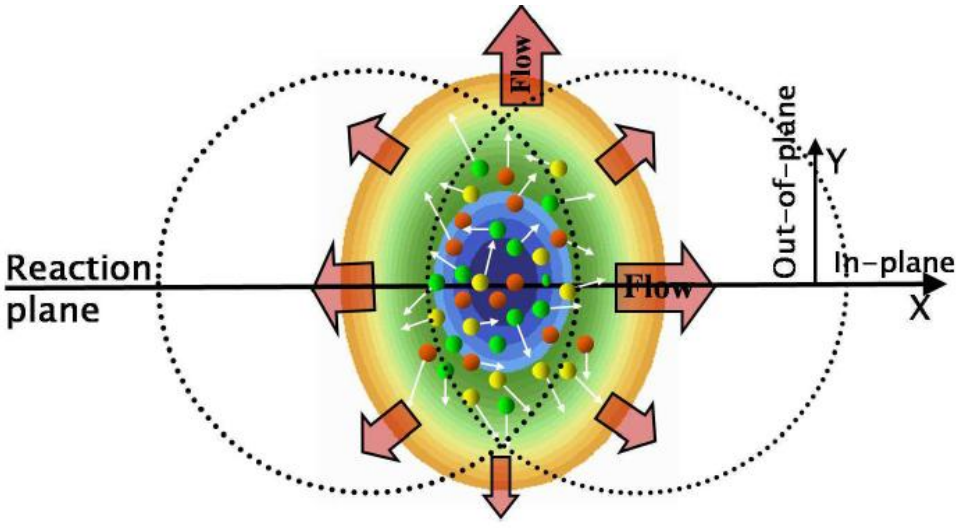

Fig. 1.5 Collective flow (in-plane and out of plane flow)

Types of flow

i) Longitudinal Flow

It describes the collective motion of the particles in their original direction defined by the beam.

ii) Radial Flow

It characterizes the azimuthal symmetric flow, observed in central collision in which the particles are emitted near $\theta_{c.m.} = 90°$ relative to beam axis.

iii) Directed Flow

The phenomenon of different fragments or different particles deflected sideward from the hot and dense region formed by the overlap of projectile and target nuclei is called directed flow. Directed flow effects mostly particles at forward and backward rapidities (at energies above a few hundred MeV/nucleon) are deflected away from beam direction by pressure built up between the colliding nuclei during the time of their mutual overlap. The effected particles quickly leaves the central region where this transverse pressure acts, the finally observed transverse flow pattern is established very easily in the collision.

iv) Elliptical Flow

It describes the azimuthal asymmetric emission pattern in which particles found to be preferentially emitted perpendicular to the reaction plane. Elliptical flow is expected to be larger in peripheral collisions.

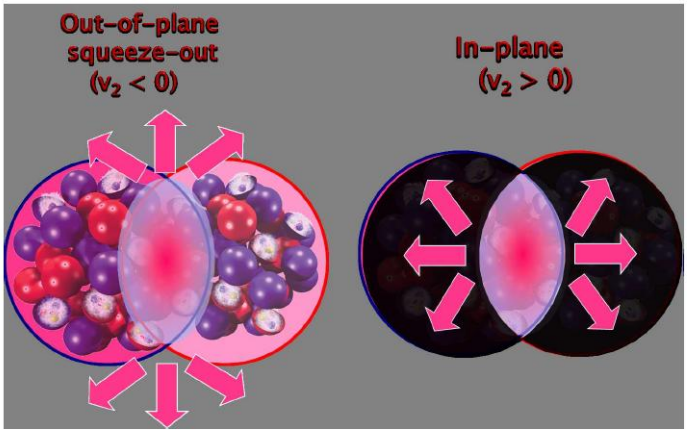

Fig. 1.6 (left) Out of plane flow and (right) in-plane flow.

1.5 Experimental Scenario

We will summarize the experiments which has been performed during recent years around the world to study heavy ion collisions (HIC).

Experiments performed at LBL in the early 80's yield first 4π information of the final momentum distributions in heavy ion reactions. The first experiment at Berkley served mainly to get experimentalists and theoreticians aware of the problems from medium energy heavy-ion collisions to equation of state. Later on, several accelerators were built at Michigan State University (USA), GANIL (France), and at GSI (Germany). These experiments enable precise measurements on the emission of primary and secondary particles and therefore provide a stimulating challenge to the theoretical description of heavy ion collisions. The SIS (Heavy-ion synchrotron) accelerator at GSI is specially designed to study the heavy-ion collisions at intermediate energies. The MSU group at Michigan State University is very active in studying the fragment's spectra at lower side of the bombarding energies. The similar efforts are also made by INDRA group at GANIL [12]. The ALADIN group at GSI has gone ahead and provided complete spectra of the fragments [13].

The FOPI and ALADIN group at GSI are studying the variety of reactions giving nearly all kinds of possibilities. It ranges from C^{12} to Pb^{208} and with incident energy between 100 MeV/nucleon and 1000 MeV/nucleon [14]. A lot of physical conclusions are also drawn from these studies. If one goes through above experiments, one will notice that two different varieties (i.e. symmetric and asymmetric reactions) merge. The symmetric reaction will generate high compression whereas asymmetric reaction will lead to heat or thermal energies. The aim of heavy target against light projectile is to look for target multifragmentation whereas a heavy projectile on light target gives projectile fragmentation. Naturally, the physics at peripheral collisions is dominated by the spectator physics whereas the central collisions have a fireball dynamics.

Different experiments gave indications that the impact parameter can be closely related with the emission of charged particles, thus make it possible to extract the impact parameter experimentally. A large multiplicity of the charged particles is associated with central collisions which decreases with increase in impact parameter [15-17]. If one deals with the intermediate mass fragment production at higher energies, one sees a rise or fall in the multiplicity of the fragments with a change in the impact parameter. Apart from these observations, the associated

properties of fragments like collective flow, energy spectra, rapidity distributions are also investigated.

The nucleons are found to be emitted from participant zone whereas the heavy fragments are the remnants of spectators. The collective flow is found to increase with increase in the size of fragments. At very low incident energies, one finds negative sideward flow whereas at high incident energies the flow is repulsive. This means that while going from low to high energies, the flow will disappear at some incident energy. This energy is termed as balance energy. It was also reported that this balance energy varies as $A^{-1/3}$ [18]. Where A is considered as sum of mass of projectile and mass of target (A= $A_T + A_P$).

1.6 Theoretical review of models

Theoretically several models have been developed to study HIC at intermediate energy. These models can be broadly divided into dynamical and statistical models are explained as follows:

a) Time Dependent Hartree-Fock (TDHF)

The conventional theories like time dependent Hartree-Fock (TDHF) [19] or its semi-classical version the so called Valsov equation (in phase space) are suitable approaches at low energies where the nucleon-nucleon collisions are negligible. A suitable approach for intermediate energy heavy-ion physics should treat the nucleon nucleon collision and mean field on equal footing. Some attempts were made in literature to extend the TDHF to take care of residual nucleon nucleon interactions which are responsible for two body collision (and dubbed as ETDHF) [20]. However due to complications, this theory could not be used for large scale investigations.

b) Boltzmann-Uehling-Uhlenbeck Model

Increasing in complexity from a single particle description mean fields can be introduced to modulate the overall behavior of nucleons. The Boltzmann-Uehling-Uhlenbeck (BUU) [21] model is able to explain one body observables like coleective flow and particle spectra nicely. Due to lack of fluctuations and correlations, the N-body predictions are beyond the scope of these models. The N-body features can be described nicely within molecular dynamics models.

c) Molecular dynamics

The classical molecular dynamics (MD) [22] approach is capable of treating both compression and fragment formation. The molecular dynamics predicts the collective flow in a qualitative

agreement with the data. It incorporates the complete classical N-body dynamics which is necessary to describe the formation of fragments. Naturally, the simple classical molecular dynamics needs refinement which should also include quantum features.

i) Quantum Molecular Dynamics Model

The QMD model [23] attempts to manipulate a many-body wave function to introduce the correlations needed for cluster formation. In past decade, several refinements and improvements were made over original QMD.

In view of the difficulties encountered with taking the Pauli principle in classical MD methods properly into account, a new class of approaches was developed in the beginning of the 1990s, the so called fermionic molecular dynamics:FMD for fermionic molecular dynamics [24] and AMD for antisymmerized molecular dynamics [25].

ii) Isospin Dependent Quantum Molecular Dynamics Model

IQMD model [26] in heavy ion collision is used for studying the isospin effects on nuclear transverse collective flow, nuclear radial flow and fragmentation.

The dynamics in the formation of the transient state is mainly governed by three components, namely, the mean field, two body collisions, and Pauli blocking. For an isospin dependent reaction dynamics algorithm it is essential that all the three components should reasonably include isospin degrees of freedom. In addition, it is also important that, in initialization of projectile and target nuclei, the samples of neutrons and protons in phase space should be treated separately since there exists a large difference between neutron and proton density distributions for nuclei. IQMD model is developed just on above basis. It has been shown that the IQMD can be used with large success for studying the effects of isospin in heavy ion collisions at intermediate energies.

Chapter 2

Methodology

2.1 Introduction

The N-body approaches are very powerful in the description of the simultaneous break-up of a nuclear system in multiple fragments, since they preserve correlations among nucleons. The classical molecular dynamics (MD) approach (or the equation of motion), in principle, is capable of treating both the compression and the fragment formation. The molecular dynamics predicts the collective (sideward) flow in a qualitative agreement with the data. It incorporates the complete classical N-body dynamics which is necessary to describe the formation of the fragments. With the passage of time QMD model is developed by taking care of the quantum features like Pauli blocking, Fermi momentum and deep inelastic scattering. Its isospin dependent version known as Isospin dependent QMD and is very successful in explaining the isospin effects in heavy ion collisions by treating the protons and neutrons explicitly.

2.2 QMD Model (Quantum molecular dynamics model)

QMD Model [23] is a n-body theory that simulates heavy-ion reactions at intermediate enegies on an event by event basis. On the basis of all fluctuations and correlations, its main advantages are:

a) Many body processes the formation of complex fragments are explicitly treated.

b) The other one is the model allows for an event by event analysis of heavy-ion reactions

QMD Model consists of mainly three step evolution:

a) Intialization

In order to generate nuclei that step is known as very first step of QMD model is “initialization”.

b) Propagation

Now, these nucleons, then propagate under the influence of surrounding mean field & the term is “propagation”.

c) Collision

Then nucleons are bound to collide if they come too close to each other and this step is known as "collision".

2.3 Isospin dependent quantum molecular dynamics model (IQMD)

The IQMD [26] model has been successfully used for the analysis of large number of observables from low to high energies. It treats different charge states of nucleons, pions and deltas explicitly as inherited from Vlasov-Uehling Uhlenbeck (VUU) model [27]. The isospin degree of freedom enters into the calculations via. symmetry potential, cross sections and Coulomb interaction. This model also includes three important steps: First, one has to generate the nuclei. This procedure is called as initialization. Successfully generated nuclei propagate under the influence of surrounding mean field. This is termed as propagation. Finally, nucleons are bound to collide if they come too close to each other. This part is dubbed as collisions. The elastic and inelastic cross-sections for proton-proton, neutron-neutron as well as proton-neutron are supposed to be affected in the presence of isospin.

a) Initialization

In this model, baryons are represented by Gaussian-shaped density distributions

$$f_i(r,p,t) = \frac{1}{\pi^2\hbar^2} e^{-(r-r_i(t))^2\frac{1}{2L}} e^{-(p-p_i(t))^2\frac{2L}{\hbar^2}} \quad (2.1)$$

Here in equation (2.1), Gaussian width L is regarded as the interaction range of the particle. The system dependence of L has been introduced in IQMD in order to obtain maximum stability of the nucleonic density profiles. For the heavier system (e.g. Au + Au), its value is chosen 8.66 fm^2,while for lighter one (i.e. Ca + Ca), the value is 4.33 fm^2.

Nucleons are initialized in a sphere with radius R = 1.12 $A^{1/3}$ fm, in accordance with the liquid drop model. Each nucleon occupies a volume of h^3, so that phase space is uniformly filled. The initial momenta are randomly chosen between 0 and Fermi momentum (p_f), without any further local constraints. The Fermi momentum p_f depends on the ground state density. For ρ_0 = 0.17 fm^{-3}, it has a value of about 268 MeV/c. Moreover, the IQMD model performs a Lorentz

contraction of the nucleus coordinate distribution, which becomes important at the higher energies.

b) Propagation

The successfully initialized nuclei are then boosted towards each other with proper center of mass velocity using relativistic kinematics. The nucleons of target and projectile interact via two and three-body Skyrme forces, a Yukawa potential and momentum dependent interactions. The isospin degree of freedom is treated explicitly by employing a symmetry potential and explicit Coulomb forces between protons of colliding target and projectile. This helps in achieving correct distribution of protons and neutrons within nucleus.

The hadrons propagate using Hamilton equations of motion:

$$\frac{dr_i}{dt} = \frac{d\langle H\rangle}{dp_i}, \frac{dp_i}{dt} = -\frac{d\langle H\rangle}{dr_i} \tag{2.2}$$

With

$$\langle \mathrm{H}\rangle = \langle \mathrm{T}\rangle + \langle \mathrm{V}\rangle \tag{2.3}$$

$$= \sum_i \frac{p_i^2}{2m_i} + \sum_i \sum_{j>i} \int f_i(r,p,t) V^{ij}(r',r)$$

$$\times f_j(r',p',t) dr dr' dp dp' \tag{2.4}$$

The baryon-baryon potential V^{ij}, in the above relation, reads as:

$$V^{ij}(r'-r) = V^{ij}_{Skyrme} + V^{ij}_{Yukawa}$$

$$+V^{ij}_{Coul} + V^{ij}_{Mdi} + V^{ij}_{Sym} \tag{2.5}$$

$$=\left(t_1\delta(r'-r) + t_2\delta(r'-r)\rho^{\gamma-1(r'+r/2)}\right)$$

$$+t_3 \frac{(\exp(-|r'-r|/\mu))}{(|r'-r|/\mu)} + \frac{Z_i Z_j e^2}{|r'-r|} +$$

$$t_4 ln^2\left[t_5\left(p_i'-p\right)^2 + 1\right]\delta(r'-r)$$

$$+ t_6 \frac{1}{\varrho_0} T_3^i T_3^j \delta\left(r_i'-r_j\right) \tag{2.6}$$

Here Z_i and Z_j denote the charges of i^{th} and j^{th} baryon, and T_3^i , T_3^j are their respective T_3components (i.e. 1/2 for protons and -1/2 for neutrons). Meson potential consists of Coulomb interaction only. The parameters μ and $t_1 \ldots t_6$ are adjusted to the real part of the nucleonic optical potential. Other baryonic potentials like V_{Skyrme}^{ij} and V_{mdi}^{ij} are isospin independent. Two different equation of states using this phenomena have been implemented. A hard equation of state with a compressibility of 380 MeV and a soft equation of state with a compressibility of 200 MeV. The Yukawa potential V_{Yuk}^{ij} is very short ranged (μ = 0.4 fm in contrast to μ = 1.5 fm in QMD) and weak.

c) Collision

Two particles collide if their minimum distance r, i.e. the minimum relative distance of the centroids of the Gaussians during their motion, in their CM frame fulfills the requirement:

$$|r_i - r_j| \leq \sqrt{\frac{\sigma_{tot}}{\pi}}, \sigma_{tot} = \sigma\left(\sqrt{s}, type\right) \tag{2.7}$$

Where "type" in equation (2.7) denotes the ingoing collision partners (N-N, N-Δ, N – π etc.). The colliding particles can also scatter elastically or inelastically. The scattering of nucleons in nuclear matter in low density expansion can be described in terms of reaction G-matrix. At high energies the influence of Pauli blocking is less and kinetic energy is large as compared to the potential. Then the imaginary part of the reaction matrix becomes identical to the transition matrix which describes the scattering between two nucleons. Scattering can be elastic or inelastic. The respective strength of different cross-sections in shown in the Fig.2.1. The total cross-section is the sum of the elastic and all inelastic cross-sections. The elastic and inelastic cross-sections for proton-proton (pp) and proton-neutron (pn) used in IQMD. The neutron-neutron (nn) cross-section is assumed to be equal to pp. The total cross-section is equal to sum of elastic and inelastic cross-section as shown in equation (2.8)

$$\sigma_{tot} = \sigma_{el} + \sigma_{inel} \tag{2.8}$$

2.4 Minimum Spanning Tree (MST) method

MST is the method used to clusterize the nucleons. In MST, two nucleons share the same fragment if their centroids are closer than a distance d_{min} ,

$$|r_i - r_j| \leq d_{min}$$

Where r_i and r_j are spatial position of both nucleons. The value of d_{min} can vary between 2-4 fm.

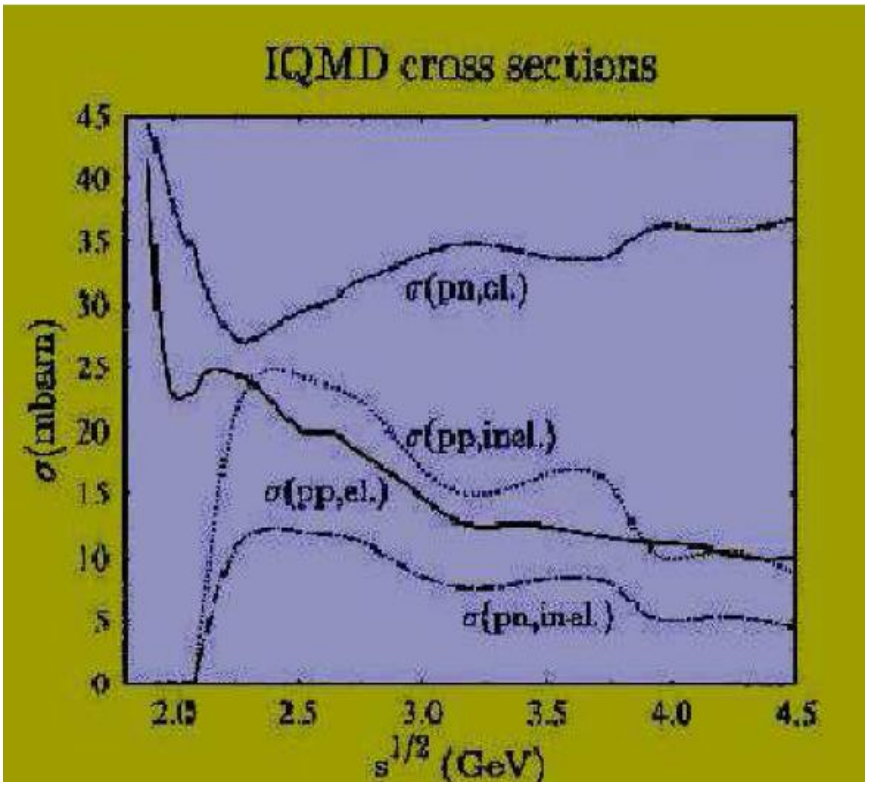

Fig. 2.1 The elastic and inelastic cross-sections for proton-proton (pp) and proton-neutron (pn) used in IQMD. The neutron-neutron cross-section is assumed to be equal to pp. The total cross-section is equal to sum of elastic and inelastic cross-section [26].

However, this method can not address the question of time scale as it will give a big fragment at the time of highest density when the interactions between the nucleons are still active. This method can only be used to analyze asymptotic configuration in which the fragmenting system can be viewed as a very dilute mixture of free particles and almost equilibrated fragments.

Chapter 3

Directed Flow and Nuclear Stopping

One of the major goal of heavy ion collision at intermediate energy is to extend the knowledge of hot and dense nuclear matter to the extreme conditions. In last decade, these studies were focused on multifragmentation that constituted fragments of all sizes. An additional promising observable for the understanding of nuclear equation of state is global stopping of nuclear matter [28]. It has been pointed out that nuclear stopping power in intermediate energy HIC (heavy ion collision) is determined by both mean field as well as in-medium nucleon-nucleon cross-section [29]. The absolute value of the stopping results from interplay between the attractive mean field and repulsive nucleon-nucleon scattering. The nuclear stopping can be used as a new probe to extract the information about correlation between the nuclear stopping and the directed flow.

3.1 Global stopping

The global stopping is defined as the randomization of one-body momentum space or memory loss of the incoming momentum. More the initial memory of nucleons erased, better it is stopped and better one has average mixing of projectile and target momentum. The destruction of initial correlations make the matter homogenous and can have global stopping.

There are four parameters used for explaining the nuclear stopping which are given as below

1. Rapidity distribution [4]

$$y(i) = \frac{1}{2} ln \frac{E(i)+p_z(i)}{E(i)-p_z(i)} \tag{3.1}$$

Where $E(i)$ and $p_z(i)$ are the total energy and longitudinal momentum of ith particle. For a complete stopping, one expects a single Gaussian shape. Obviously, narrow Gaussian indicate better thermalization compared to broader Gaussian.

2. The second probe of the degree of stopping is the anisotropy ratio <R> :

$$\langle R \rangle = \frac{2}{\pi} \frac{\sum_i |p_\perp(i)|}{\sum_i |p_\parallel(i)|} \tag{3.2}$$

Where, summation runs over all nucleons. The transverse and longitudinal momenta are

$p_\perp(i) = \sqrt{p_x^2(i) + p_y^2}(i)$ and $p_\parallel(i) = p_z(i)$ respectively. Naturally, for a complete stopping, $\langle R \rangle$ should be equal to unity.

3. The third quantity which is known as indicator of nuclear stopping and is known as Quadrupole moment & is given by:

$$Q_{zz} = \sum_i (2p_z^2(i) - p_x^2(i) - p_y^2(i)) \quad (3.3)$$

For complete stopping Q_{zz} should be equal to zero.

4. The forth parameter is varxz [30] which is the ratio of the variance of longitudinal and transverse rapidity distributions.

$$\text{Varxz} = \frac{\sigma^2(y_x)}{\sigma^2(y_z)} \quad (3.4)$$

3.2 Transverse in-plane flow

Collective transverse in-plane flow has also been studied for last three decades and used to explore the isospin dependence of equation of state (EOS). For transverse flow we use the quantity directed transverse momentum $< P_x^{dir} >$ which is defined as:

$$< P_x^{dir} > = \frac{1}{A} \sum_{i=1}^{A} sign\{y(i)\} p_x(i) \quad (3.5)$$

The energy dependence of collective flow led its disappearance [31] at balance energy. Disappearance of flow at particular energy called energy of vanishing flow or balance energy [31].

From the above discussions of stopping parameters and transverse in-plane flow one can see that these are related to one another. As at the point where flow vanishes, the nuclear stopping will be maximum. Experimentally, this connection is studies by Reisdorf *et. al.* [30] by using scaled directed flow and varxz. In the present work our aim is to study the different aspects of stopping parameters and $<P_x^{dir}>$ such as excitation function, system size dependence and effect of colliding geometry. Moreover, it would be of great interest to study the correlation between these parameters for symmetric reactions.

3.3 Results and discussion

For the present analysis simulations have been carried out for the reactions of $^{40}_{20}Ca_{20}$ + $^{40}_{20}Ca_{20}$, $^{58}_{28}Ni_{30}$ + $^{58}_{28}Ni_{30}$, $^{83}_{36}Kr_{47}$ + $^{83}_{36}Kr_{47}$ and $^{124}_{47}Ag_{77}$ + $^{124}_{47}Ag_{77}$ at an incident energy from 100 to 600 MeV/nucleon for the scaled impact parameter $\hat{b} = \frac{b}{b_{max}}$ = 0.1 to 0.5, where b_{max} = 1.12 ($A_T^{1/3} + A_P^{1/3}$) fm (A_T and A_P are mass of target and projectile respectively). The phase space generated by the IQMD model has been analyzed using the minimum spanning tree method. The MST [6] method binds two nucleons in a fragment if their distance in coordinate space is less than 4 fm.

As we are interested in studying the correlation between the nuclear stopping and the directed flow. One has to understand <dN/dY> as a function of $y_{c.m.}/y_{beam}$ at different energies and impact parameters. To this end, we display in Figs. 3.1 & 3.2 the <dN/dY> as a function of $y_{c.m.}/y_{beam}$ at different impact parameters (Fig. 3.1) and at different energies (Fig. 3.2) for two different cross-sections isospin dependent (σ_{iso}) ($\sigma_{np} = 3\sigma_{nn} = 3\sigma_{pp}$) and isospin independent (σ_{noiso}) ($\sigma_{np} = \sigma_{nn} = \sigma_{pp}$).

The parameter $y_{c.m.}/y_{beam} = 0$ corresponds to the mid rapidity (participant) zone and, hence, is responsible for hot and compressed zone. On the other hand, $y_{c.m.}/y_{beam} \neq 0$ corresponds to spectator zone, $y_{c.m.}/y_{beam} < -1$ corresponds to target-like (TL) and $y_{c.m.}/y_{beam} > 1$ corresponds to projectile like (PL) distributions.

3.3.1 Rapidity distribution as a function of $y_{c.m.}/y_{beam}$

a) at different impact parameters

Fig.3.1, displays the rapidity distribution as a function $y_{c.m.}/y_{beam}$ at an incident energy 100 MeV/nucleon at different scaled impact parameter. Left panels shows the rapidity distribution for isospin dependent cross-section (σ_{iso}) and right panels shows the rapidity distribution for isospin independent cross-section (σ_{noiso}). From top to bottom panels shows the mass dependent of rapidity distribution. One can see that, as we increase the impact parameter the participant matter goes on decreasing which leads to the decrease in stopping. It has been observed that the

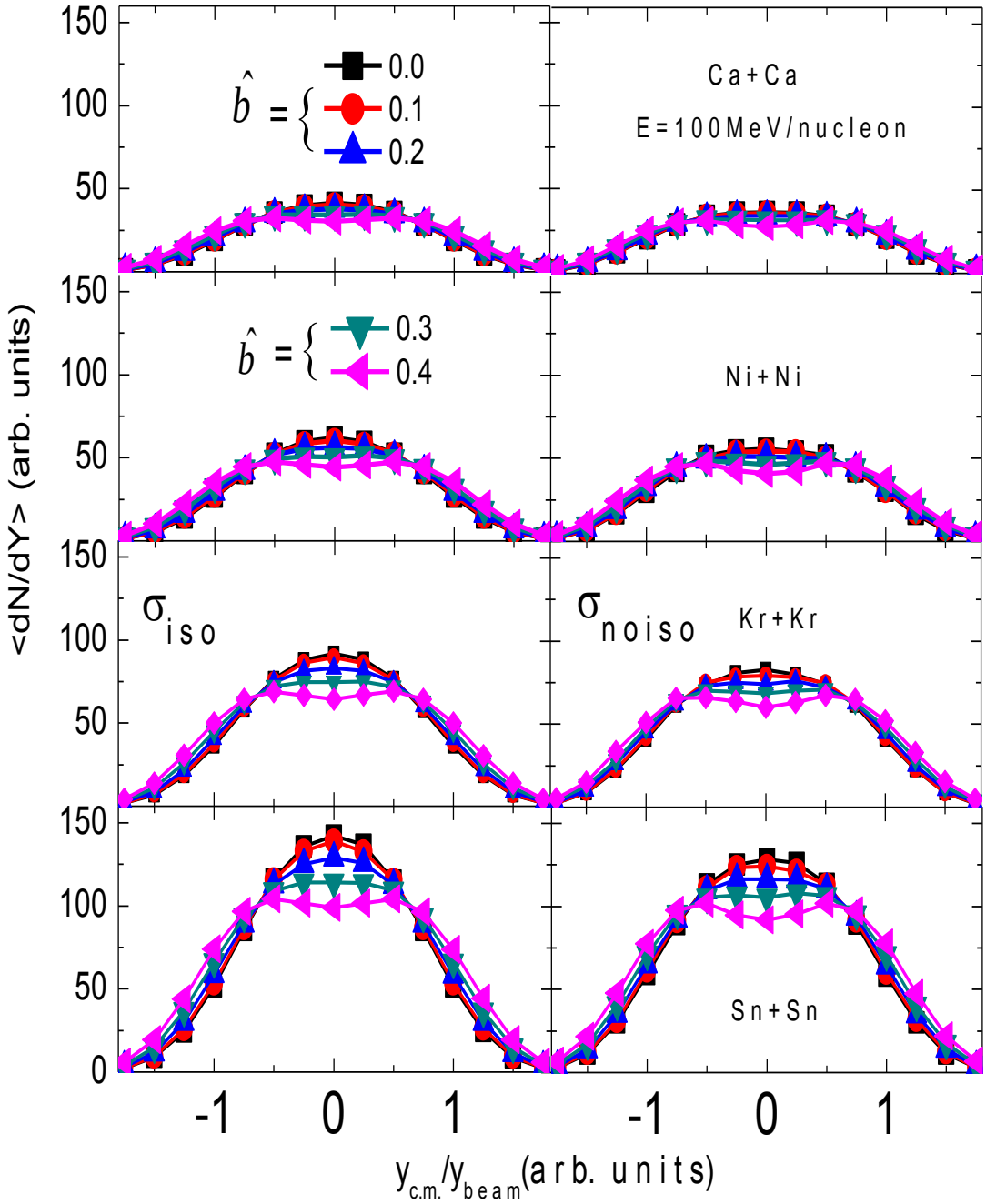

Fig.3.1 Rapidity distribution <dN/dY> as a function of $y_{c.m.}/y_{beam}$ at different scaled impact parameter.

lighter systems shows the broader Gaussian shape than heavier systems. Cross-section shows a little influence on the rapidity distribution. In case of isospin dependent cross-section we observe the narrow gausian. Thus the heavier systems are better thermalized than lighter one.

b) at different energies

Fig.3.2, shows the result for rapidity distribution <dN/dY> as a function of $y_{c.m.}/y_{beam}$ at energy an incident energy range 100 MeV/nucleon and 400 MeV/nucleon for isospin dependent (left panels) and for isospin independent (right panels) cross-sections. Thus Since the collision is semiperipheral, we get the projectile (towards negative) and target (towards positive) like distributions. As the participant matter decreases the thermalization also decreases. Moreover, the lighter systems are lesser thermalized than heavier systems because of reduction in participant zone for systems. For system mass dependent of rapidity distribution is similar as explained in case of Fig.3.1. Also in this figure the better thermalization is observed in case of isospin dependent cross-section σ_{iso} .

3.3.2 Variation of stopping parameters and directed flow

a) As a function of energy

Fig.3.3, displays the results for the variation of the stopping parameters (anisotropy ratio and quadrupole moment) and directed flow with energy. From figure it has been observed that the anisotropy ratio and quadrupole moment decreases with increase in energy. This happens because transverse momentum components decreases with incident energy. But the directed flow increases with increase in incident energy. This happens because for symmetry reactions the binary collisions increases with incident energy. At lower incident energy, the dominance of the attractive mean field produces the negative flow where as frequent nucleon-nucleon collisions and repulsive mean field at high incident energy results in positive flow. Thus with increase in incident energy there will be large transverse flow of nucleons due to dominant coulomb repulsion.

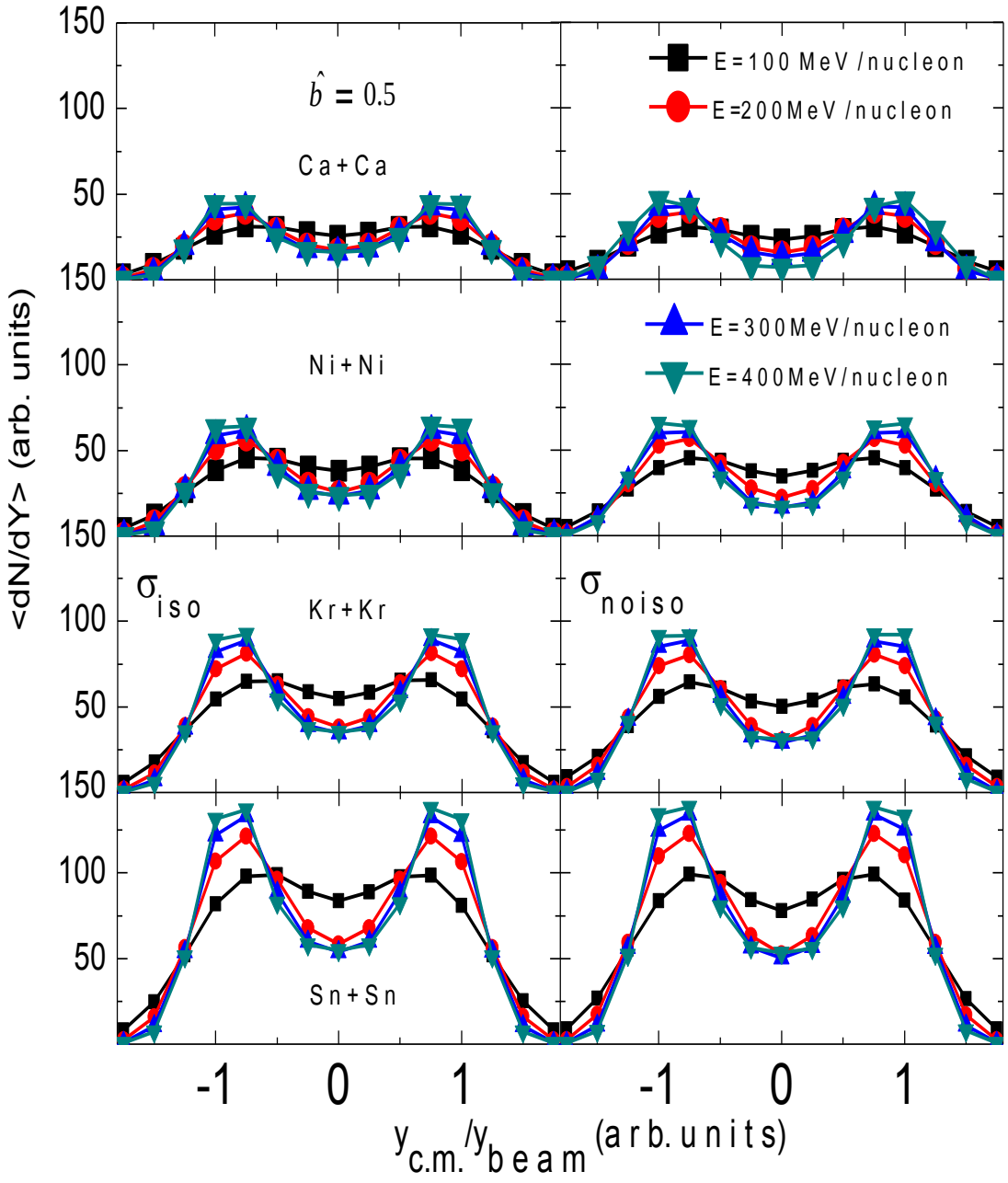

Fig.3.2 Rapidity distribution <dN/dY> as a function of $y_{c.m.}/y_{beam}$ at different energies.

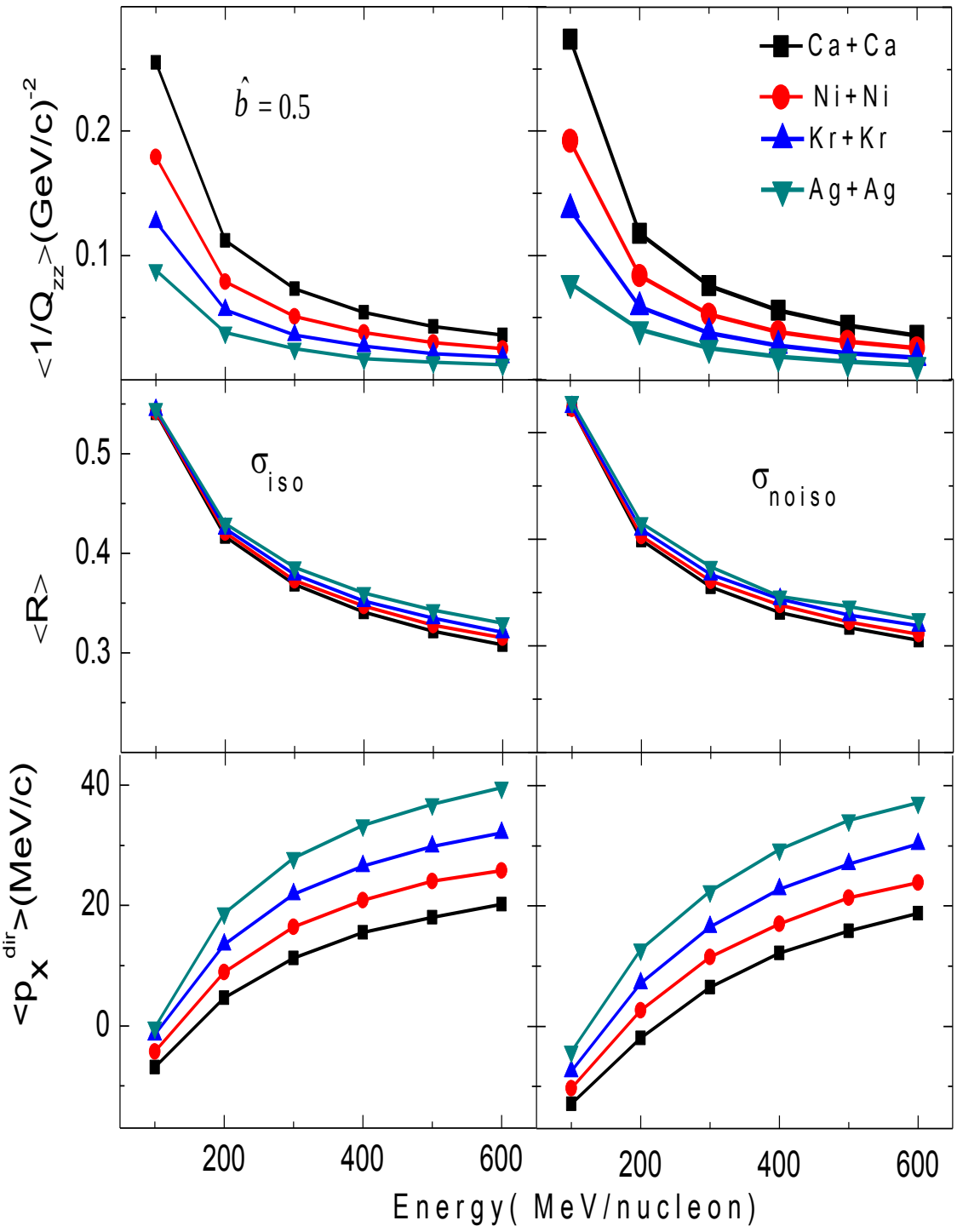

Fig.3.3 Variation of stopping parameter <R>, <1/Q_{zz}> and directed flow with energy.

b) As a function of impact parameters

We display in Fig.3.4, the impact parameter dependence of the stopping parameters and directed flow. The results are displayed at incident energy 100 MeV/nucleon. It has been observed that the parameters <R> and $< 1/Q_{zz} >$ behave in a similar manner. The amount of stopping decreases with increase in the impact parameter. Reduced participant matter is the cause for this decrease. The value of stopping is more for σ_{iso} than for σ_{noiso} . This happens because isospin dependent cross-section will lead to violent nucleon-nucleon collisions which causes better theramlization. On comparing the value of stopping for all systems we found that heavier mass systems give better thermalization than lighter systems. The directed flow shows the opposite behavior compared to stopping observables. As stopping variables are going to decrease, the directed flow increases with increase in impact parameter. This is due to decreased participant zone in peripheral collisions which decreases the amount of repulsive nucleon-nucleon collisions for lighter systems. To overcome this effect higher energy is required. This kind of effect is less pronounced in heavier systems as significant nucleon-nucleon collisions occur in these systems. It has been observed that due to increased nucleon-nucleon repulsion the effected nucleons moves in transverse direction away from participant zone.

3.3.3 Variation of stopping parameters with system mass

a) At different impact parameter

In Fig.3.5, we displays the variation of stopping variables with system mass at different scaled impact parameters for different systems for isospin dependent (left panels) and isospin independent (right panels) cross-sections. One can see that the stopping decreases with increase in the impact parameter. This happens because Participant matter decreases with increase in impact parameter and thus the stopping decreases.

b) At different energies

Fig,3.6, shows the results for variation of stopping parameters and directed flow with system mass at different energies from 100 MeV/nucleon to 600 MeV/nucleon. With increase in the incident energy, the stopping parameters decreases. For isospin dependent cross-section we observe the better thermalization than isospin independent cross-section

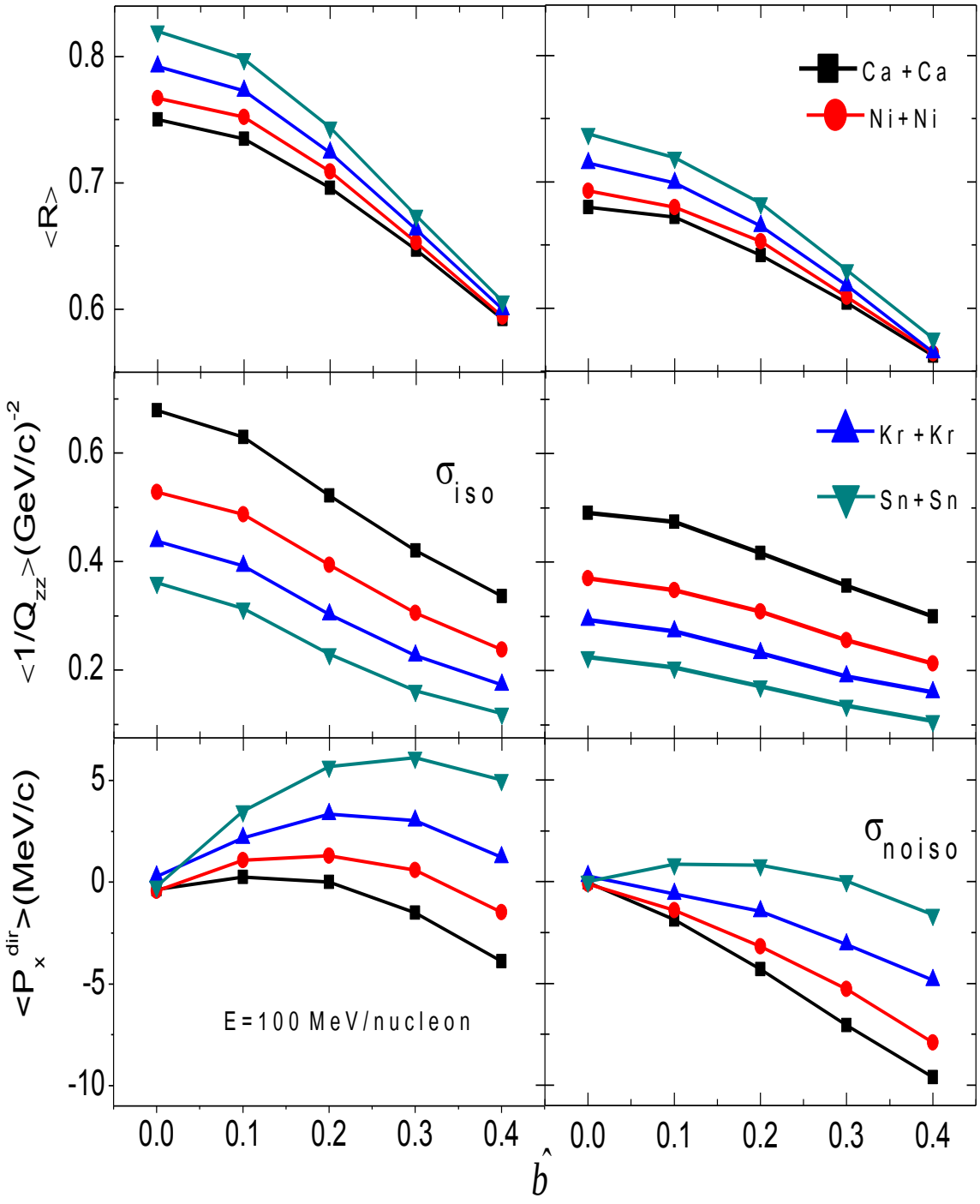

Fig.3.4 Variation of stopping parameters and directed flow as a function of impact parameter

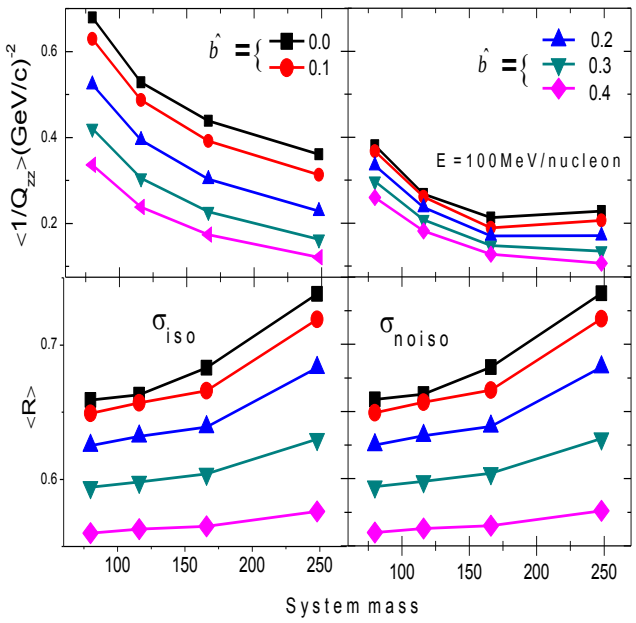

Fig.3.5 variation of stopping parameters with system mass at different impact parameter

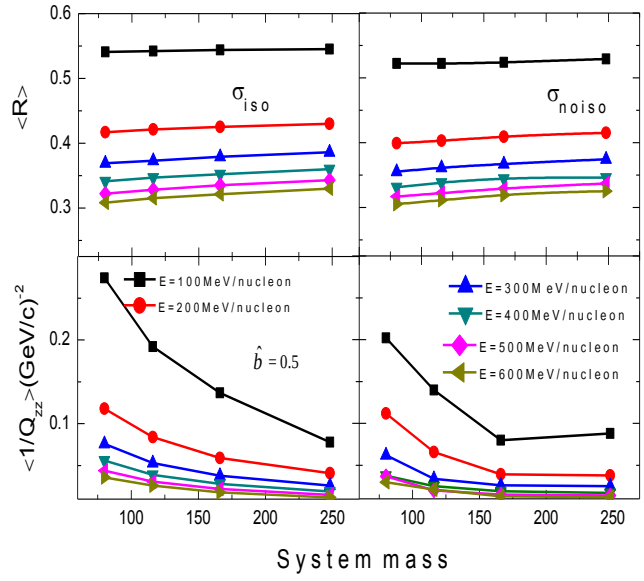

Fig.3.6 Variation of stopping parameters with system mass at different energies

3.3.4 Correlation between stopping and directed flow

Fig.3.7, shows the variation of directed flow as a function of stopping observable < R > at different incident energies for different systems. It has been observed that directed flow and the stopping observable shows a linear relationship and shows a positive going slope at each value of energy.

3.3.5 System size dependence of varxz

To study the effect of system size on varxz, we display in Fig.3.8, the system size dependence of varxz. Theoretical results are compared with the experimental findings of FOPI collaboration. We display here the results of varxz for Au + Au, Ca + Ca, Ni +Ni, Ru + Ru and Xe + Xe in central collisions. One can see that the varxz increases with increase in system size. It has been observed that for heavier systems the value of varxz < 1 i.e. even for central collisions the systems are not fully thermalized and is considered as evidence of partial transparency, rather than the dominance of longitudinal over transversal pressure gradients.

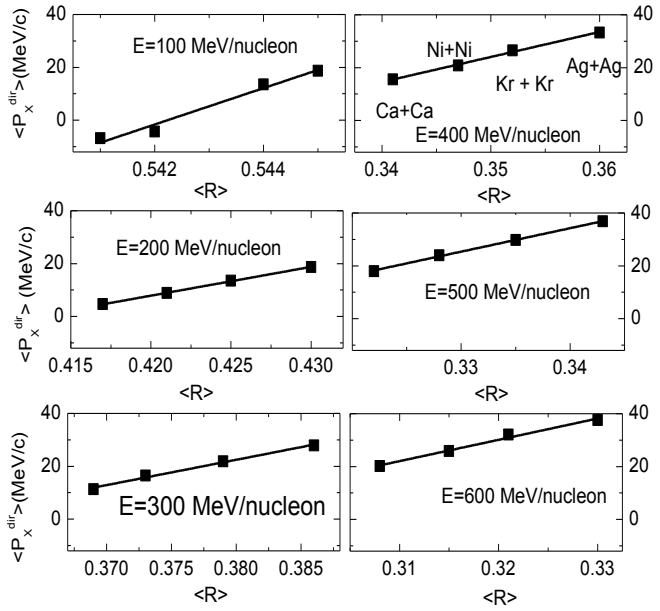

Fig.3.7 corrlation between stopping and directed flow.

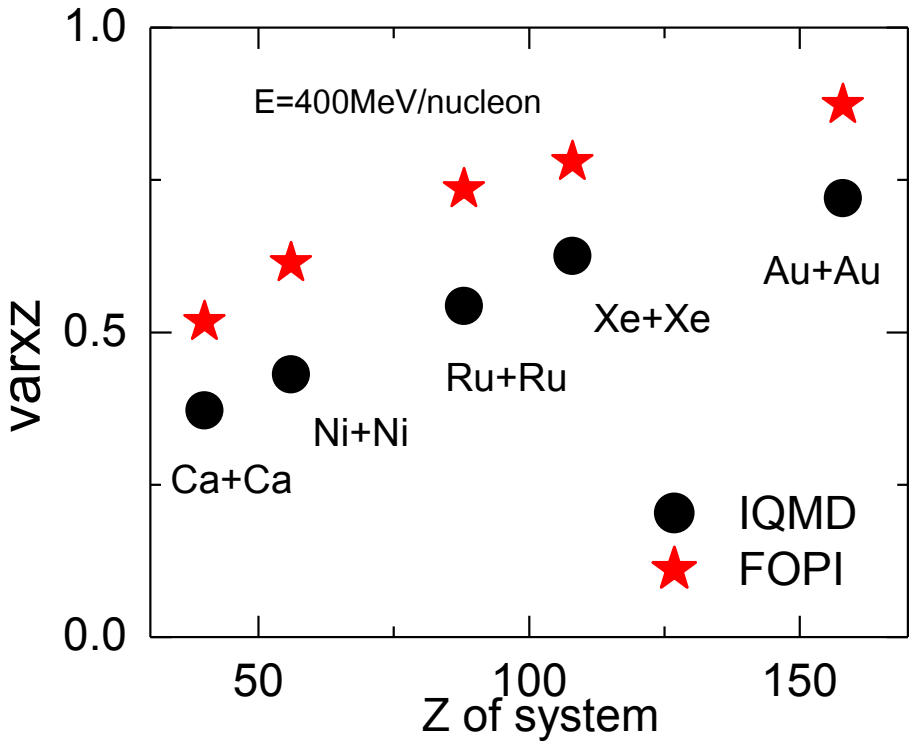

Fig.3.8 system size dependence of varxz.

3.4 Summary

The dissertation contains a theoretical study of nuclear stopping and transverse flow in heavy ion collisions at intermediate energy. The IQMD model is used to study the nuclear stopping and directed flow for $^{40}_{20}Ca_{20}$ + $^{40}_{20}Ca_{20}$, $^{58}_{28}Ni_{30}$ + $^{58}_{28}Ni_{30}$, $^{83}_{36}Kr_{47}$ + $^{83}_{36}Kr_{47}$ and $^{124}_{47}Ag_{77}$ + $^{124}_{47}Ag_{77}$ at E = 100 to 600 MeV/nucleon and scaled impact parameter $\hat{b}$ = 0.0, 0.1, 0.2, 0.3, 0.4. The detailed study of theoretical models were discussed in chapter 2.

In chapter 3, we have attempted to understand the nature of nuclear stopping and directed flow for different systems at wide range of energies and impact parameters. The effect of isospin dependent and isospin independent cross-sections has also been studied. Also, the correlation between nuclear stopping and directed flow has been studied and the results for varxz compared with the experimental data of FOPI collaboration.

References

[1] W. Scheid, R. Ligensa, and W. Greiner. Phys. Rev. Lett. **21**, 1479 (1968).

[2] R. B. Clare and D. Strottman. Phys. Rep. **141**, 179 (1986).

[3] R. Stock. Phys. Rep. **135**, 261(1986).

[4] S. Kumar, S. Kumar, R. K. Puri, Phys. Rev. C **81**, 014611(2010).

[5] S. Kumar, V. Kaur, R. K. Puri, Nucl. Phys. A **861** (2011).

[6] Y. K. Vermani, R. K. Puri, Eur. Phys. Lett. **85**, 62001(2009).

[7] S. Terranova and A. Bonasera, Phys .Rev. C **70**, 024906 (2004).

[8] S. Kumar, S. Kumar, R.K. Puri, Phys. Rev. C **78**,064602 (2008).

[9] W. Bauer, Phys. Rev. Lett. **61**, 2534 (1988).

[10] Y. Yano, Nucl. Inst. Meth. B **261**, 1009 (2007).

[11] B. A. Li, C.M. Ko, Nucl. Phys. A **601**,457 (1996).

[12] J. D. Frankland *et al*., Phys. Rev. C **71**, 034607 (2005).

[13] A. S. Botvina *et al*., Phys. Rev. C **74**, 044609 (2006).

[14] M. Begemann-Blaich *et al*., Phys. Rev. C **48**, 610 (1993).

[15] T. Li *et al*., Phys. Rev. Lett. **70**, 1924 (1993).

[16] M. B. Tsang *et al*., Phys. Rev. Lett. **71**, 1502 (1993).

[17] R. T. de Souza *et al.,* Phys. Rev. Lett. **268**, 6 (1991).

[18] V. de la Mota *et al.,* Phys. Rev. C **46**, 677 (1992).

[19] H. Stocker and W. Greiner, Phys. Rep. **137**, 277(1986).

[20] E. Suraud, Ch. Gregoire and B. Tamain, Prog. Part. Nucl. Phys. **23**, 357 (1989).

[21] F. Giacosa, T. Gutsche, and A. Faessler, Phys. Rev. C **71**, 025202 (2005).

[22] A. R. Bodmer, C. N. Panos and A. D. Mackellar, Phys. Rev. C **22**, 1025 (1980); L. Wilets, Y. Yariv and R. Chestnut, Nucl. Phys. A **301**, 359 (1970).

[23] J. Aichelin, Phys. Rep. **202**, 233 (1991).

[24] H. Feldmeier, Nucl. Phys. A **515**, 147 (1990); J. Schnack, Ph. D. Thesis, GSI report, Darmstadt (1996); H. Feldmeir, K. Beller, Proc. I. Europ. Biennial Work-shop on Nucl. Phys., Megeve, France, World Scientific, S. 125 (1991); K. Beiler, Diplomarbeit, TH Darmstadt (1991).

[25] A. Bohnet, N. Ohtsuka, J. Aichelin, R. Linden and A. Faessler, Nucl. Phys. A **494**, 349 (1989).

[26] C. Hartnack et al., Eur. Phys. J. A **1**, 151 (1998).

[27] W. Bauer, Phys. Rev. Lett. **61**, 2534 (1988).

[28] L. Q. Feng and L. Z. Xia, Chin. Phys. Lett. **19**, 321 (2002).

[29] W. Bauer, Phys. Rev. Lett. **61**, 2534 (1988).

[30] W. Reisdorf et al. , Phys. Rev. Lett. **92**, 232301 (2004) ; T. Gaitanos, C. Fuchs and H. H. Wolter Phys. Lett. B **609**, 241 (2005).

[31] S. Gautam et al., J. Phys. G: Nucl. Part. Phys. **37**, 085102 (2010); S. Gautam and A. D. Sood, Phys. Rev. C **82**, 014604 (2010).